



Enhanced adaptive DA-ML carrier phase estimator and its application to accurate laser linewidth and SNR estimation

YAN LI,^{1,2} TIANYU SONG,^{1,*} MOHAN GURUSAMY,¹ CHANGYUAN YU,³ AND POOI-YUEN KAM^{1,2}

¹Department of Electrical and Computer Engineering, National University of Singapore, 117583, Singapore

²National University of Singapore (Suzhou) Research Institute, 215123, China

³Department of Electronic and Information Engineering, Hong Kong Polytechnic University, Hong Kong
*song.tianyu@u.nus.edu

Abstract: We proposed a novel adaptive carrier phase estimator based on the phase information of the received signal only. Through eliminating the perturbation due to the amplitude of the AWGN, the proposed method outperforms the conventional adaptive filter in terms of both the carrier phase estimation and the filter gain tracking. Additionally, a dynamic tracking of both the laser linewidth and SNR is derived based on the proposed carrier phase estimator which requires no prior knowledge of the channel parameters. Numerical simulations and experiments are conducted to verify its feasibility in real applications.

© 2018 Optical Society of America under the terms of the [OSA Open Access Publishing Agreement](#)

OCIS codes: (060.4510) Optical communications; (060.1660) Coherent communications.

References and links

1. K.-P. Ho, *Phase-Modulated Optical Communication* (Springer US, 2005), 1st ed.
2. R. Noe, "PLL-free synchronous QPSK polarization multiplex/diversity receiver concept with digital I&Q baseband processing," *IEEE Photonics Technol. Lett.* **17**, 887–889 (2005).
3. A. J. Viterbi and A. M. Viterbi, "Nonlinear estimation of PSK-modulated carrier phase with application to burst digital transmission," *IEEE Trans. Inf. Theory* **29**, 543–551 (1983).
4. D. S. Ly-Gagnon, S. Tsukamoto, K. Katoh, and K. Kikuchi, "Coherent detection of optical quadrature phase-shift keying signals with carrier phase estimation," *J. Lightwave Technol.* **24**, 12–21 (2006).
5. P. Kam, "Maximum likelihood carrier phase recovery for linear suppressed-carrier digital data modulations," *IEEE Trans. Commun.* **34**, 522–527 (1986).
6. P. Y. Kam, K. H. Chua, and X. Yu, "Adaptive symbol-by-symbol reception of mpsk on the gaussian channel with unknown carrier phase characteristics," *IEEE Trans. Commun.* **46**, 1275–1279 (1998).
7. S. Zhang, P. Y. Kam, C. Yu, and J. Chen, "Decision-aided carrier phase estimation for coherent optical communications," *J. Lightwave Technol.* **28**, 1597–1607 (2010).
8. C. C. Chan, *Optical performance monitoring: advanced techniques for next-generation photonic networks* (Academic Press, 2010).
9. D. R. Pauluzzi and N. C. Beaulieu, "A comparison of snr estimation techniques for the awgn channel," *IEEE Trans. Commun.* **48**, 1681–1691 (2000).
10. Y. Yu, B. Dong, and C. Yu, "Optical signal-to-noise ratio monitoring using a Sagnac interferometer based on fiber birefringence," *IEEE Photonics Technol. Lett.* **27**, 1899–1902 (2015).
11. D. Derickson, "Fiber optic test and measurement," in "Fiber optic test and measurement/edited by Dennis Derickson. Upper Saddle River, NJ: Prentice Hall, c1998.", (1998).
12. T. Sutuli, R. C. Figueiredo, and E. Conforti, "Laser linewidth and phase noise evaluation using heterodyne offline signal processing," *J. Lightwave Technol.* **34**, 4933–4940 (2016).
13. H. Fu and P. Y. Kam, "Phase-based, time-domain estimation of the frequency and phase of a single sinusoid in awgn—the role and applications of the additive observation phase noise model," *IEEE Trans. Inf. Theory* **59**, 3175–3188 (2013).
14. E. Ip and J. M. Kahn, "Feedforward carrier recovery for coherent optical communications," *J. Lightwave Technol.* **25**, 2675–2692 (2007).
15. Q. Wang and P. Y. Kam, "Optimum detection of two-dimensional carrier modulations with linear phase noise using received amplitude and phase information and performance analysis," *J. Lightwave Technol.* **34**, 2439–2451 (2016).
16. R. Maher and B. Thomsen, "Dynamic linewidth measurement technique using digital intradyne coherent receivers," *Opt. Express* **19**, B313–B322 (2011).

17. Z. Zan and A. J. Lowery, "Experimental demonstration of a flexible and stable semiconductor laser linewidth emulator," *Opt. Express* **18**, 13880–13885 (2010).

1. Introduction

To comply with the enormous requirements on the bandwidth, the application of the advanced modulation formats, like M -ary phase shift keying (MPSK) and M -ary quadrature amplitude modulation (MQAM), in coherent optical fiber communication systems has received much attention. However, coherent detection of phase modulation suffers from the impairments of additive white Gaussian noise (AWGN), as well as the laser phase noise induced by the transmitter and receiver lasers [1]. Hence, carrier phase estimation (PE) prior to coherent detection is indispensable. A phase-locked loop (PLL) is one candidate for carrier phase tracking. However, due to the large product of laser linewidth and loop delay, the PLL combined with the distributed feedback laser is difficult to use [2]. Early receivers also use the conventional M th power carrier phase estimator for coherent optical M -ary phase shift keying (MPSK) [3, 4]. Due to the use of nonlinear operations, like the M th power, this method incurs high computational complexity. The decision-aided maximum likelihood (DA-ML) phase estimator is another effective candidate [5]. However, the selected estimation window length would affect the accuracy of the estimated carrier phase. The adaptive DA-ML phase estimator is further derived in [6, 7] to avoid the block length effect, but the amplitude of the received signal considered in this algorithm deviates the convergence of the phase estimation.

Meanwhile, to maintain the control of network elements and improve the fault management, optical performance monitoring (OPM) is essential particularly in complex communication networks [8]. Conventionally, performance management involves measurements of system parameters such as the optical power, system noise level and wavelength. Among them, the signal-to-noise ratio (SNR) is one of the most important parameters in terms of evaluating the signal quality. Moreover, many techniques, such as adaptive coding and soft decoding, require *a priori* knowledge of SNR. The maximum likelihood (ML) SNR estimator is commonly used [9]. However, its performance is highly sensitive to the phase noise. The optical signal processing based methods using Mach-Zehnder delay interferometer and Sagnac interferometer are efficient candidates for SNR estimation [10]. However, optical signal processing require additional hardware, which may be inapplicable due to practical limitations and cost.

The characterization of the laser phase noise due to the transmitter and receiver lasers attracts extensive investigations as well. Early researchers relied on the electrical spectrum analyzer for accurate estimation of laser linewidth [11]. Recently, coherent receiver based techniques, which allows time-domain digital signal processing (DSP), become more popular. Both static and dynamic estimation can be performed using either heterodyne or intradyne receiver [12].

This paper focuses on the dynamic tracking of the symbol SNR and laser linewidth by using DSP based method. The carrier phase estimation performance would strongly affect the tracking accuracy of the channel parameters. Previously, the adaptive DA-ML carrier phase estimator is a powerful candidate [6, 7]. In our recent work, we realize that the amplitude of the received signal, which is still considered in the conventional adaptive DA-ML method, is irrelevant to the carrier phase tracking [13]. In this paper, we propose an enhanced version of the adaptive DA-ML estimator, in which the amplitude part of the received signal is not used. With the new method, both filter gain and decision-based techniques for dynamic tracking of SNR and laser linewidth are derived and evaluated through numerical simulation and experiments.

2. Enhanced adaptive DA-ML carrier phase estimator

2.1. Signal Model In Coherent Receiver

In this paper, we start from a linear phase noise-dominant channel with perfectly compensated chromatic dispersion, polarization mode dispersion and frequency offset [7]. The received signal model is given as

$$r(k) = m(k)e^{j\theta(k)} + n(k). \quad (1)$$

Here, $m(k)$ denotes the k -th transmitted symbol, which takes on values from the signal set $\{S_i = A(i)e^{j\phi(i)}, i = 0, 1, 2, \dots, M-1\}$ with equal probability. $A(i)$ and $\phi(i)$ denote the amplitude and phase modulation of each symbol. M denotes the number of signal points. Term $n(k)$ is a complex, Gaussian random variable with mean zero and variance N_0 , where N_0 is the double-sided spectrum density of the AWGN. E_s denotes the average power per symbol. For multiple level constellations, the amplitude of transmitted signal can be further expressed as

$$A(i) = \rho_i \sqrt{E_s}, \quad (2)$$

where ρ_i denotes the weight coefficient and $M = \sum_{i=0}^{M-1} \rho_i^2$. Term $\theta(k)$ denotes the laser phase noise due to the transmitter and receiver lasers. As in [14], the carrier phase $\theta(k)$ is commonly modeled as a Wiener process

$$\theta(k) = \sum_{m=-\infty}^k v(m), \quad (3)$$

where $\{v(m)\}$ is a set of independent and identically distributed (i.i.d.), Gaussian random variables with mean zero and variance of

$$\sigma_p^2 = 2\pi\Delta\nu T. \quad (4)$$

T and $\Delta\nu$ denote the symbol duration and combined linewidth of transmitter and receiver lasers, respectively. Moreover, the phase noise increment sequence $\{v(k)\}_k$ and the AWGN sequence $\{n(k)\}_k$ are mutually independent.

2.2. Conventional Adaptive DA-ML Method

Based on (1), for coherent demodulation, the elimination of the carrier phase $\theta(k)$ is required prior to the decision procedure. Previously, researchers rely on the DA-ML method, where a sequence of previous decisions is used to estimate the carrier phase of current symbol. In DA-ML method, with the assumption of slowly varying carrier phase, the carrier phase estimation of k th symbol can be achieved by maximizing the likelihood function of L previous received symbols $\{r(l)\}_{l=k-L}^{k-1}$. However, simulation results show that, the selected window length would affect the estimation accuracy [7]. To eliminate the block length effect, the adaptive DA-ML carrier phase estimator is proposed in [6]. Instead of using a window, the phase estimation is derived by minimizing a risk function of all passed symbols.

Here, the reference phase (RP) at $k+1$ -th symbol $V(k+1)$ is defined as

$$V(k+1) = \alpha V(k) + (1-\alpha)r(k)/\hat{m}(k), \quad (5)$$

where $\hat{m}(k)$ denotes the hard decision of $m(k)$. Commonly, we assume that $V(k) \approx e^{j\hat{\theta}(k)}$ particularly at high SNR, where $\hat{\theta}(k)$ denotes the estimation of the carrier phase $\theta(k)$. Through minimizing the conditional risk function $R(k)$ given in [6]

$$R(k) = E \left[\sum_{l=1}^k |r(l) - V(l)\hat{m}(l)|^2 \middle| \{r(l)\}_{l=1}^k \right], \quad (6)$$

the filter gain α at each time k can be calculated as

$$\alpha(k) = \frac{A(k)}{B(k)}, \quad (7)$$

where

$$\begin{aligned} A(k) &= A(k-1) + \sum_{l=1}^k |\hat{m}(l)|^2 \\ &\quad \cdot [|g(l-1)|^2 - \Re[V(l-1)g^*(l-1) - g(l)[V^*(l-1) - g^*(l-1)]]] \\ B(k) &= B(k-1) + \sum_{l=1}^k |\hat{m}(l)|^2 \cdot |V(l-1) - g(l-1)|^2 \\ g(k) &= \frac{r(k)}{\hat{m}(k)}. \end{aligned} \quad (8)$$

While operating the adaptive filter given in (5), the initial condition of $\alpha(0) = 0$ and $V(0) = 1$ is chosen to give the maximum gain of 1 to the first received symbol.

In real applications, the implementation of the adaptive DA-ML method would inevitably lead to phase reference error (PRE) which is defined as $\theta_e(k) = \theta(k) - \hat{\theta}(k)$. It has been shown that at high SNR and low laser linewidth, θ_e is approximately Gaussian distributed with mean zero and variance [7]

$$\sigma_e^2 = \frac{\sigma_p^2}{1 - \alpha^2} + \frac{\eta}{2\gamma_s} \frac{1 - \alpha}{1 + \alpha}. \quad (9)$$

Here $\gamma_s = E_s/N_0$ denotes the average symbol SNR and $\eta = E[1/|m(k)|^2]$ denotes the constellation penalty [14]. According to the simulation results provided in [7], with $\sigma_p^2 = 3.41 \times 10^{-4} \text{rad}^2$, the measured PRE variance agrees very well with the theoretical value given in (9) at γ_s greater than 10 dB for M-PSK and 15 dB for 16QAM. Additionally, if the SNR and laser linewidth can not guarantee the assumption of the Gaussian distribution of $\theta_e(k)$, the carrier phase estimator still works, except that the PRE variance will not agree so closely with the analytical result. From (9), the optimum steady-state α , denoted by α_o , can be easily calculated by minimizing the PRE variance, which gives

$$\alpha_o = 1 + \frac{\gamma_s \sigma_p^2}{\eta} - \frac{\gamma_s \sigma_p^2}{\eta} \sqrt{\frac{2\eta}{\gamma_s \sigma_p^2} + 1}. \quad (10)$$

During the implementation, the calculated α is expected to converge to the optimal steady-state value α_o . According to (10), α_o is a function of the laser phase noise variance σ_p^2 , symbol SNR γ_s and constellation penalty η . Therefore, with known system parameters, the convergence of α can be facilitated by substituting the calculated α_o into (5) as the initial value of α . However, simulation results show that, there exists a gap between the theoretical α_o calculated from (10) and the steady-state α measured from simulation [6], which would block the implementation of α_o in real applications. This is because, in (5), assuming perfect hard decision, i.e. $\hat{m}(k) = m(k)$, the adaptive DA-ML phase estimation can be written as

$$V(k+1) = \alpha(k)V(k) + [1 - \alpha(k)] \left[e^{j\theta(k)} + \frac{n(k)}{m(k)} \right]. \quad (11)$$

From (11), obviously, $n(k)$ and $m(k)$ are independent of the carrier phase $\theta(k)$ of current symbol. Hence, term $n(k)/m(k)$ would lead to negative perturbations to the carrier phase estimation and further slow down the convergence of the adaptive filter gain α . To mitigate the negative perturbation, we propose an enhanced adaptive DA-ML phase estimator where the amplitude part of the noise term $n(k)/m(k)$ is filtered out.

2.3. Enhanced adaptive DA-ML phase estimator

For better phase estimation, in the enhanced method, we make use of a new variable $m'(k) = |r(k)|e^{j\hat{\phi}(k)}$ to eliminate the amplitude noise due to the AWGN, which gives

$$V_E(k+1) = \alpha_E V_E(k) + (1 - \alpha_E) \frac{r(k)}{m'(k)}. \quad (12)$$

Here, $\hat{\phi}(k)$ denote the decision of the phase modulation $\phi(k)$. Similarly, the filter gain α_E at each time k can be calculated by minimizing the conditional risk function given in (6), which gives

$$\begin{aligned} \alpha_E(k) &= \frac{A_E(k)}{B_E(k)} \\ A_E(k) &= A_E(k-1) + \sum_{l=1}^k |m'(l)|^2 \\ &\quad \cdot [|g_E(l-1)|^2 - \Re [V_E(l-1)g_E^*(l-1) - g_E(l) [V_E^*(l-1) - g_E^*(l-1)]]] \\ B_E(k) &= B_E(k-1) + \sum_{l=1}^k |m'(l)|^2 \cdot |V_E(l-1) - g_E(l-1)|^2 \\ g_E(k) &= \frac{r(k)}{m'(k)}. \end{aligned} \quad (13)$$

Similar with that in conventional adaptive filter, the initial value of $\alpha(0)$ and $V(0)$ while applying the enhanced method is chosen as 0 and 1, respectively.

Considering perfect hard decision, we have $\hat{\phi}(k) = \phi(k)$. Substituting (1) into (12), we have

$$V_E(k+1) = \alpha_E V_E(k) + (1 - \alpha_E) e^{j[\theta(k) + \epsilon(k)]}, \quad (14)$$

where $\epsilon(k)$ denotes the additive observation phase noise (AOPN) due to the AWGN $n(k)$ [15]. It has been shown that at high SNR, Tikhonov distributed $\{\epsilon(k)\}$ can be approximated as a sequence of independently distributed Gaussian random variables with mean zero and variance

$$\sigma_\epsilon^2 = \eta/2\gamma_s. \quad (15)$$

Similarly, the phase of the RP calculated from (14) is recognized as the carrier phase estimation. Considering the PRE of the enhanced adaptive DA-ML method, we have

$$e^{j(\theta(k+1) - \theta_e(k+1))} = \alpha_E e^{j(\theta(k) - \theta_e(k))} + (1 - \alpha_E) e^{j[\theta(k) + \epsilon(k)]}. \quad (16)$$

Dividing both sides of (16) by $e^{j\theta(k)}$ and applying the approximation: $e^{jx} \approx 1 + jx$, we have

$$\theta_e(k+1) = \nu(k+1) + \alpha_E \theta_e(k) - (1 - \alpha_E) \epsilon(k). \quad (17)$$

Taking the expectation of the both sides, we have

$$E[\theta_e(k+1)] = E[\nu(k+1)] + \alpha_E E[\theta_e(k)] - (1 - \alpha_E) E[\epsilon(k)] = \alpha_E E[\theta_e(k)]. \quad (18)$$

Considering the initial phase estimation error $\theta_e(0)$, we have

$$E[\theta_e(0)] = E[\theta(0)] - E[\hat{\theta}(0)] = E[\nu(0)] - E[\angle[V(0)]]. \quad (19)$$

Since the initial value of $V(0)$ is chosen as 1, we have

$$E[\theta_e(0)] = E[\nu(0)] - E[\angle[1]] = 0. \quad (20)$$

Substituting (20) into (18), we can easily find that $E[\theta_e(k)] = 0$. The PRE variance, $\text{var}[\theta_e(k)]$, can be obtained by squaring the both sides of (17) and taking the expectation. Note that $\theta_e(k)$ given in (17) depends on $\{\nu(l)\}_{l=1}^{k-1}$, while $\{\nu(l)\}_l$ is a sequence of independent, identically distributed random variables. Hence, $\theta_e(k)$ and $\nu(k+1)$ are mutually independent. Moreover, the AOPN term $\epsilon(k)$ depends only on the AWGN $n(k)$, where the AWGN sequence $\{n(k)\}_k$ is independent of the phase noise increment $\{\nu(k)\}_k$. Thus, $\theta_e(k)$ and $\nu(k+1)$ are independent of $\epsilon(k)$. In this case, through squaring (17), the PRE variance can be written as

$$\text{var}[\theta_e(k+1)] = \alpha_E^2 \text{var}[\theta_e(k)] + \sigma_p^2 + (1 - \alpha_E)^2 \sigma_\epsilon^2. \quad (21)$$

The steady-state PRE variance $\sigma_e^2 = \lim_{k \rightarrow \infty} \text{var}^2[\theta_e(k)]$ can be calculated by solving (21) with $\text{var}^2[\theta_e(k+1)] = \text{var}^2[\theta_e(k)]$, which gives

$$\sigma_e^2 = \frac{\sigma_p^2}{1 - \alpha_E^2} + \frac{\eta}{2\gamma_s} \frac{1 - \alpha_E}{1 + \alpha_E}. \quad (22)$$

Note that the PRE variance of the enhanced filter given in (22) is the same as that of the conventional one given in (9). This is because, during the derivation of the PRE variance, we consider the assumption of high SNR where the amplitude noise due to the AWGN is less significant. Hence, the conventional adaptive DA-ML method achieves similar performance with the enhanced method. In this case, both the conventional filter and its enhanced version share the same optimal steady-state α_o as derived in (10). However, due to the elimination of the amplitude noise, the proposed enhanced phase estimator is expected to achieve better estimation accuracy compared with the conventional one at relatively low SNR. Additionally, without the deviation due to the amplitude noise, the actual filter gain measured from the enhanced phase estimator would converge closer to the optimal α_o calculated from (10).

3. SNR and laser linewidth estimation

3.1. Filter gain-based method

The accurate tracking of the adaptive filter gain α by using the enhanced adaptive phase estimator enables the estimation of both combined laser linewidth and symbol SNR. As shown in (10), the steady-state filter gain α_o is a function of the symbol SNR γ_s and laser phase noise variance σ_p^2 . During the implementation, the α_o can be estimated by averaging the calculated α over a long period of time after reaching the steady-state. Hence, with known SNR γ_s , the laser phase noise variance σ_p^2 can be calculated by inverting (10), which gives

$$\sigma_p^2 = \frac{\alpha_o^2 - 2\alpha_o + 1}{2\alpha_o} \frac{\eta}{\gamma_s}. \quad (23)$$

The combined laser linewidth can be further calculated as $\Delta\nu = \sigma_p^2/2\pi T$. Similarly, with known $\Delta\nu$, the symbol SNR can be calculated by solving (10), which gives

$$\gamma_s = \frac{\alpha_o^2 - 2\alpha_o + 1}{2\alpha_o} \frac{\eta}{\sigma_p^2}. \quad (24)$$

However, with filter gain based method, the laser linewidth $\Delta\nu$ is required when estimating the SNR γ_s and vice versa. In practical applications, the prior knowledge of the system parameters might be unavailable. To solve this problem, a simple decision based simultaneous tracking of SNR γ_s and laser linewidth $\Delta\nu$, which requires no prior knowledge, is derived as follow.

3.2. Development of the decision-based method

With accurate phase tracking by using the enhanced adaptive phase estimator, a simultaneous tracking of γ_s and $\Delta\nu$ can be obtained based on the decisions of previous symbols. In this method, after the carrier phase estimation and hard decision, the carrier phase $\theta(k)$ and phase modulation $\phi(k)$ of the received symbol can be easily removed, thereby generating an AWGN dominant estimation variable $D(k)$. Assuming perfect hard decision, we define $D(k)$ as

$$D(k) = r(k)e^{-j[\phi(k)+\hat{\theta}(k)]}. \quad (25)$$

Substituting (1) into (25) and taking the real part of $D(k)$, we have

$$D_{Re}(k) = \Re[D(k)] = \Re[\rho(k)\sqrt{E_s}e^{j\theta_e(k)} + n(k)e^{-j(\hat{\theta}(k)+\phi(k))}], \quad (26)$$

where $\Re[x]$ denotes the real part of the complex variable x . Since $|\theta_e(k)| \ll 1$, the approximation $e^{jx} \approx 1 + jx$ is applied in (26), thereby giving

$$D_{Re}(k) \approx \rho(k)\sqrt{E_s} + \Re[n'(k)], \quad (27)$$

where $n'(k) = n(k)e^{-j(\hat{\theta}(k)+\phi(k))}$. Since $n(k)$ is circular symmetric, $n'(k)$ is statistically identical to $n(k)$ which is Gaussian distributed with mean zero and variance N_0 . As aforementioned, the transmitted signal $m(k)$ is equally selected from the signal set. Hence the amplitude coefficient $\rho(k)$ follows a uniform distribution. Its mean value $\bar{\rho} = E[\rho(k)]$ can be easily calculated for a known constellation. Note that $\rho(k)$ and $n'(k)$ are independent. Taking the expectation of the both sides of (27), we have

$$E[D_{Re}(k)] = \bar{\rho}\sqrt{E_s} + E[\Re[n'(k)]] = \bar{\rho}\sqrt{E_s}. \quad (28)$$

With known $\bar{\rho}$, the average symbol energy E_s can be easily calculated from (28), which gives

$$E_s = [E[D_{Re}(k)]/\bar{\rho}]^2. \quad (29)$$

Subtracting the amplitude modulation from (27) and taking the variance, we can obtain the noise power N_0 , given as

$$N_0 = 2 \times \text{var} \left[D_{Re}(k) - \rho(k)\sqrt{E_s} \right]. \quad (30)$$

Combining (29) and (30), the symbol SNR can be simply calculated as

$$\gamma_s = \frac{[E[D_{Re}(k)]/\bar{\rho}]^2}{2 \times \text{var} \left[D_{Re}(k) - \rho(k)\sqrt{E[D_{Re}(k)]/\bar{\rho}} \right]} \quad (31)$$

Compared with the filter gain based SNR estimation given in (24), the decision-based SNR estimation given in (31) requires no prior knowledge of the laser linewidth $\Delta\nu$.

The measurement of $\{D(k)\}$ can be applied to estimate the laser linewidth $\Delta\nu$ as well. Denoting the imaginary part of $D(k)$ as $D_{Im}(k)$, we have

$$D_{Im}(k) = \Im[D(k)] = \Im[\rho(k)\sqrt{E_s}e^{j\theta_e(k)} + n'(k)], \quad (32)$$

where $\Im[x]$ denotes the imaginary part of the complex variable x . Applying the approximation: $e^{jx} \approx 1 + jx$, we can linearize (32) as

$$D_{Im}(k) = \sqrt{E_s}\rho(k)\theta_e(k) + \Im[n'(k)]. \quad (33)$$

Note that the PRE $\theta_e(k)$ is independent of the amplitude coefficient $\rho(k)$. Hence, the expectation of $D_{Im}(k)$ can be simplified as

$$\begin{aligned} E[D_{Im}(k)] &= \sqrt{E_s}E[\rho(k)\theta_e(k)] + E[\Im[n'(k)]] \\ &= \sqrt{E_s}E[\rho(k)]E[\theta_e(k)] + E[\Im[n'(k)]] = 0. \end{aligned} \quad (34)$$

The variance of $D_{Im}(k)$ can be expressed as

$$\sigma_I^2 = \text{var}[D_{Im}(k)] = E[D_{Im}(k)^2]. \quad (35)$$

Squaring both sides of (32), we have

$$D_{Im}(k)^2 = E_s\rho(k)^2\theta_e(k)^2 + \Im[n'(k)]^2 + 2\sqrt{E_s}\rho(k)\theta_e(k)\Im[n'(k)]. \quad (36)$$

Since $\rho(k)$, $n'(k)$ and $\theta_e(k)$ are mutually independent, substituting (36) into (35), we have

$$\sigma_I^2 = E_sE[\rho(k)^2]E[\theta_e(k)^2] + E[\Im[n'(k)]^2] + 2\sqrt{E_s}E[\rho(k)]E[\theta_e(k)]E[\Im[n'(k)]]. \quad (37)$$

Since the PRE of the enhanced adaptive DA-ML method $\theta_e(k)$ and $n'(k)$ are shown to be Gaussian distributed with mean of zero, we have

$$E[\theta_e(k)^2] = \sigma_e^2, \quad E[\Im[n'(k)]^2] = \text{var}[\Im[n'(k)]] = \frac{N_0}{2}. \quad (38)$$

Substituting (38) into (37), the variance of the imaginary part of $D(k)$ can be simplified as

$$\sigma_I^2 = \sigma_e^2 E_s + \frac{N_0}{2}. \quad (39)$$

Considering the PRE variance of the enhanced adaptive DA-ML method derived in (22), obviously, σ_I^2 given in (39) is a function of average symbol power E_s , noise power N_0 , symbol SNR γ_s , filter gain α and laser phase noise variance σ_p^2 . With known parameters, we can easily calculate σ_p^2 through inverting (39), which gives

$$\sigma_p^2 = (1 - \alpha_E^2) \left[\frac{\sigma_I^2}{E_s} - \frac{\eta}{2\gamma_s} \frac{1 - \alpha_E}{1 + \alpha_E} - \frac{1}{2\gamma_s} \right]. \quad (40)$$

With the σ_p^2 estimated from (40), we can calculate the laser linewidth by inverting (4), which gives

$$\Delta\nu = \sigma_p^2 / 2\pi T. \quad (41)$$

3.3. Implementation of the decision based method

During the implementation, from the definition given in (25), a series of measurements of $D(k)$ can be easily collected at the receiver side. Through averaging the real part of $D(k)$ over a long period of time, we can calculate its sample mean $\hat{E}[D_{Re}(k)]$, which can be recognized as an approximation of $E[D_{Re}(k)]$. Additionally, for a given constellation, the mean value of the amplitude coefficient $\bar{\rho}$ is known as a constant. With $\bar{\rho}$ and $\hat{E}[D_{Re}(k)]$, the signal power E_s can be easily estimated from (29). With the estimated E_s and measured $D_{Re}(k)$, we can further estimate the noise power N_0 from (30) by using the sample variance of the measurement $[D_{Re}(k) - \bar{\rho}(k)\sqrt{E_s}]$. Combining the estimated signal power and noise power, we can finally estimate the SNR γ_s .

Similarly, considering the laser linewidth estimation, the steady-state filter gain α_E can be obtained by averaging the measurements of $\alpha_E(k)$ after reaching the steady-state. Moreover, the constellation penalty η is a known parameter for a given constellation. The variance of the imaginary part of $D(k)$, σ_I^2 , can be simulated with the sample variance of $D_{Im}(k)$ measured at the receiver side. Substituting the measured γ_s from (31) into (40), we can easily calculate the phase noise variance σ_p^2 and further measure the laser linewidth $\Delta\nu$ from (41).

4. Results and discussions

4.1. Simulation

Here, Monte Carlo simulations are performed to evaluate the feasibility of the proposed enhanced adaptive DA-ML carrier phase estimator. The conventional adaptive filter is simulated for comparison. The mean square error (MSE), defined as

$$\text{MSE} = \frac{1}{N} \sum_{i=1}^N \left(\theta(i) - \hat{\theta}(i) \right)^2 \quad (42)$$

is used as the performance metric. Term $\hat{\theta}(i)$ denotes the estimated carrier phase of i th symbol and N is the number of measurements used for each calculation of the MSE. Here, the sample size is chosen as $N = 500000$ per simulation run to stabilize the simulation results. For better observation, we consider the inverse logarithmic scale of the measured MSE while plotting the figures. In Fig. 1, the MSE is measured as a function of symbol SNR γ_s by using different carrier phase estimators. As shown, compared with the conventional adaptive filter, the enhanced method achieves better carrier phase estimation performance, particularly at low SNR for all tested situations. With SNR greater the 15 dB for both 8PSK and 16QAM, the performance improvement through applying the enhanced method is less observable. This is because, at high SNR, the amplitude of received symbols is approximately static. Compared with 8PSK, performance improvement due to the enhanced method is more significant in 16QAM. This is because, in 16QAM, the amplitude fluctuation due to the multi-level modulation would disturb the phase tracking as well. In this case, the mitigation of the amplitude noise by using the enhanced method is more important. Considering the laser linewidth, similar trend in terms of the carrier phase estimation performance can be observed with different $\Delta\nu$. Moreover, the estimation accuracy decreases along with the increase of $\Delta\nu$ as we expected. With the precise tracking of the carrier phase, we will later show that the proposed phase estimator enables an accurate measurement of both SNR and laser linewidth based on either the filter gain or decisions of previous symbols.

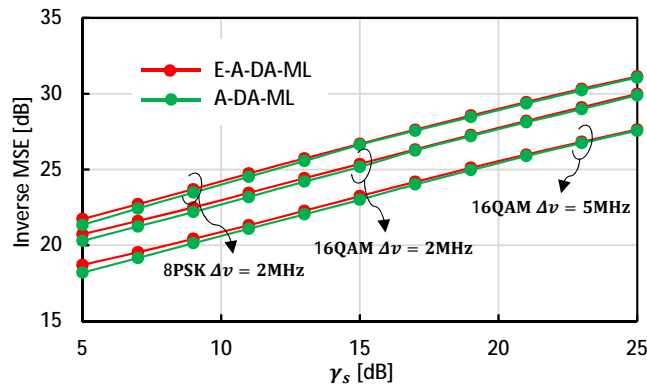


Fig. 1. Inverse MSE of the phase estimation versus the symbol SNR γ_s with symbol rate $R = 50$ G Symbols/second.

In terms of the tracing accuracy of the optimal steady-state filter gain α_o , significant performance improvement can be achieved by using the enhanced adaptive filter. Here, the inverse of the normalized mean square error (NMSE) of the measured α_o , defined as

$$\text{NMSE} = \frac{1}{N} \sum_{i=1}^N \left(\frac{\hat{\alpha}_i - \alpha_o}{\alpha_o} \right)^2, \quad (43)$$

is used as the performance metric. Term $\hat{\alpha}_i$ denotes the i th estimation of the α_o and N is the number of measurements used for each calculation of the NMSE. To ensure the estimation accuracy, we choose the sample size of $N = 100000$ during the simulation. As illustrated in Fig. 2, compared with the conventional adaptive filter, more than 10 dB performance improvement can be achieved by using enhanced method in both 8PSK and 16QAM. Compared with the 8PSK, better tracking accuracy of the steady state filter gain α can be achieved in 16QAM modulated systems with both conventional and enhanced adaptive filter. This is because, in both conventional and enhanced adaptive filter, the filter gain α is calculated through minimizing the risk function $R(k)$ given in (6), which is related to the residual amplitude and phase noise. Compare with 8PSK, 16QAM modulated systems suffer larger residual noise, which facilitates the convergence of α . Moreover, while considering the enhanced filter, since the amplitude fluctuation in 16QAM due to both the AWGN and amplitude modulation is mitigated, the performance difference compared with the 8PSK is less significant.

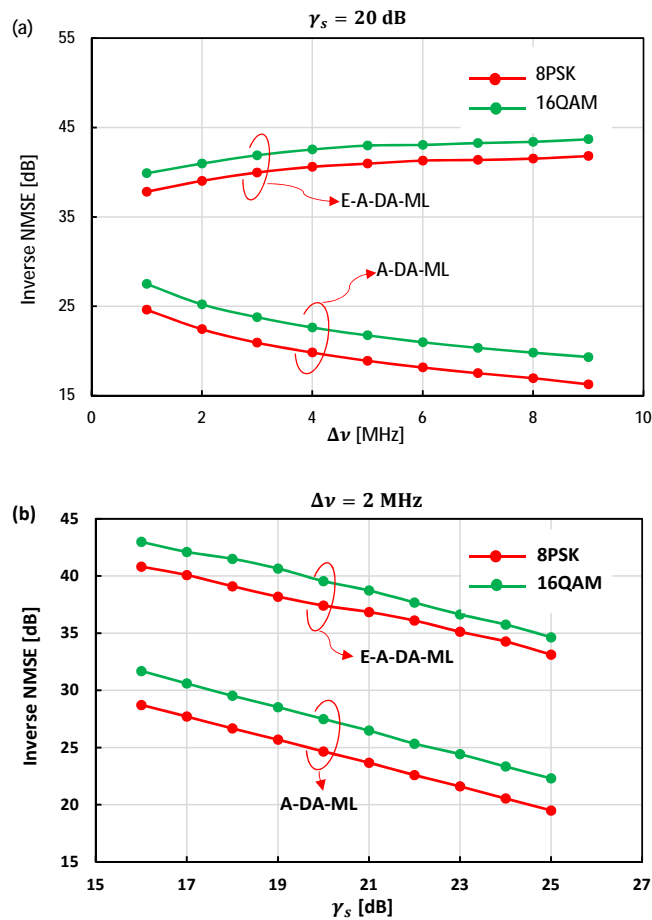


Fig. 2. Inverse NMSE of measured α versus (a) combined laser linewidth $\Delta\nu$ and, (b) symbol SNR γ_s .

In addition, as shown in Fig. 2(a), with the enhanced filter, we can observe a slight performance increase along with the increase of laser linewidth $\Delta\nu$. In contrast, as shown in Fig. 2(b), the growth of SNR γ_s degrades the tracking accuracy of the steady state α_o . This is because, with large SNR, less residual noise of previous symbols would lead to a slower convergence of α compared with that using a small SNR. Similar performance trend can be observed in [7] (Fig. 5).

In addition, here, the NMSE is applied as the performance metric. From Eq. (10), we can easily find that the calculated α_o decreases with the increase of γ_s , which further degrades the NMSE performance. Similarly, the large residual noise due to the laser linewidth $\Delta\nu$ would facilitate the convergence of α while using the enhanced adaptive method as shown in Fig. 2(a). However, with the conventional adaptive filter, since the amplitude noise would strongly disturb the convergence of α , its tolerance to the laser linewidth is less efficient compared with the enhanced method.

The enhanced adaptive filter enables, as well, an accurate estimation of the combined laser linewidth $\Delta\nu$ and symbol SNR γ_s . Both the filter gain based technique and the decision based method are tested in 8PSK and 16QAM systems with $R = 50$ G Symbols/second. For performance comparison, the instantaneous frequency based laser linewidth estimation and ML SNR estimator are tested in the same situation [9, 16]. Here, the normalized mean square error (NMSE), illustrating the relative estimation error performance, is commonly used as the performance metric [9, 16]. Similar with that in the investigation of the α tracking performance, the sample size of $N = 100000$ is used for both SNR and laser linewidth estimation.

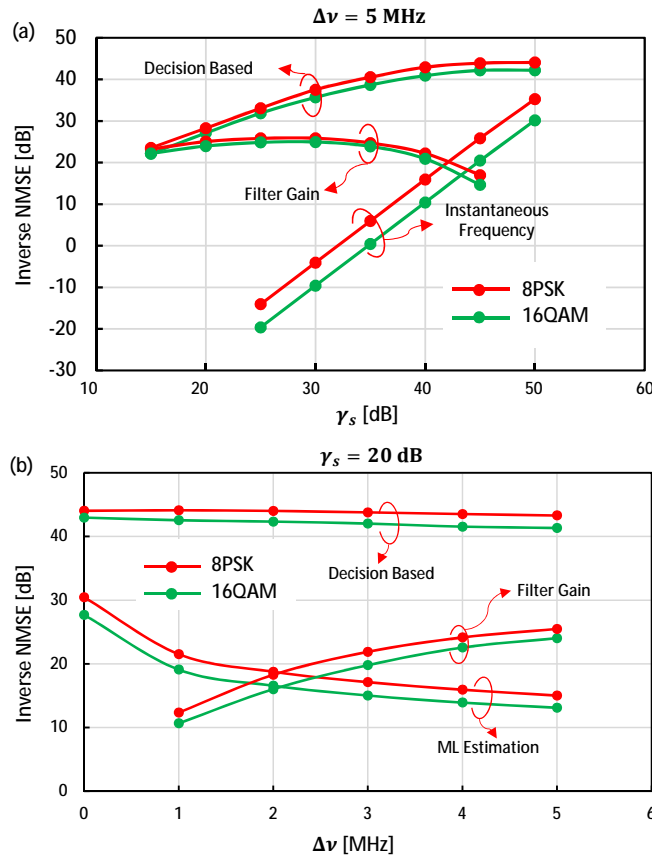


Fig. 3. Performance comparison of different (a) laser linewidth estimation methods, and (b) symbol SNR estimation techniques.

The inverse NMSE of the laser linewidth estimation using different methods are depicted in Fig. 3 as a function of the symbol SNR. Simulation results show that both the decision and filter gain based methods outperform the instantaneous frequency based method. Moreover, the instantaneous frequency based method relies highly on the SNR, while with our proposed methods, 20 dB inverse NMSE can be obtained at $\gamma_s = 15$ dB. Compared with the filter gain based method, estimation using the symbol decision achieves better performance in all tested

constellations. Additionally, with the increase of γ_s , a continuous performance improvement can be observed by using the decision based methods. In contrast, while using the filter gain based method, the increase of γ_s leads to the decrease of the tracking accuracy of the steady-state filter gain α_o , thereby leading to performance degradation on the laser linewidth estimation.

The performance of multiple SNR estimators are tested in both 8PSK and 16QAM systems. As shown in Fig. 3(b), the inverse NMSE of the SNR estimation are measured as a function of the laser linewidth $\Delta\nu$. Obviously, the decision based SNR estimator achieves best estimation accuracy in all considered constellations within the entire range of $\Delta\nu$ tested. Considering the filter gain based estimator, we can observe a continuous performance increase along with the growth of $\Delta\nu$. Additionally, simulation results show that the filter gain based technique outperform the conventional ML estimator particularly at large laser linewidth. This is because the ML method is proposed without the consideration of the phase noise. During our simulation, the use of the enhanced adaptive DA-ML phase estimator would lead to inevitable PRE, thereby generating negative effects on the performance of the ML estimator.

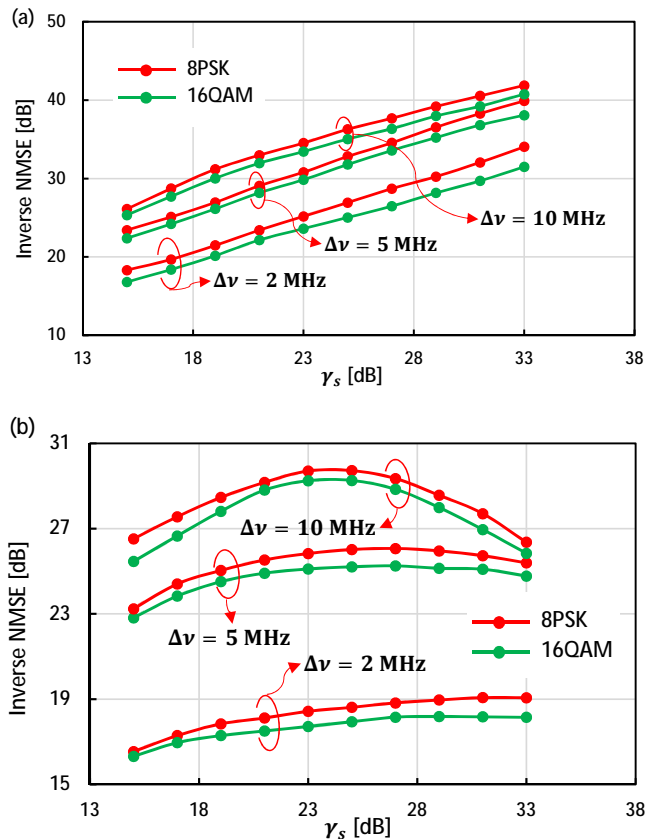


Fig. 4. Performance investigation of (a) decision and, (b) filter gain based laser linewidth estimators.

For comprehensive performance investigation, the proposed laser linewidth estimators are investigated in 50 G Symbols/second 8PSK and 16QAM systems within a wide range of SNR and laser linewidth. As shown in Fig. 4, the increase of $\Delta\nu$ improves the estimation performance in both filter gain and decision based techniques. In decision based estimator, high SNR leads to less fluctuation on the measured sample mean and variance of the decision variable $D(k)$. Therefore, a performance improvement can be observed with the growth of γ_s . In contrast, there exists an optimal SNR value with minimum NMSE in filter gain based laser linewidth estimator

particularly at high $\Delta\nu$. This is because, in filter gain based method, the laser linewidth estimation performance is closely related to the tracking accuracy of α . As mentioned above, the increase of SNR will degrade the convergence speed of α , thereby generating certain amount of bias in laser linewidth estimation and decreasing the estimation performance. However, the increase of γ_s also mitigates the fluctuation of the estimated laser linewidth. Hence, at $\Delta\nu=10$ MHz, we can still observe a performance improvement at SNR below around 23 dB. However, after reaching the optimal point, the AWGN no longer dominates. In this case, the mitigation of the estimation noise due to the AWGN is less important. Hence, the increasing bias at high SNR degrades the estimation accuracy. Additionally, as shown in Fig. 4(b), the optimal SNR increases with the decrease of the laser linewidth. This is because, with smaller $\Delta\nu$, the estimation noise fluctuation due to the laser phase noise is less significant. Hence, the elimination of the AWGN induced estimation noise is more important compared that considering a large $\Delta\nu$.

The SNR estimation performance of various methods are illustrated in Fig. 5 as a function of laser linewidth and SNR. Similarly, the filter gain based technique achieves better performance at larger $\Delta\nu$. In contrast, the increase of $\Delta\nu$ degrades the estimation accuracy of the decision based technique. This because the large PRE as a result of a large laser linewidth value would conflict with the approximation applied during the derivation of the decision based SNR estimator. Moreover, an optimal SNR value can be observed in both filter gain and decision based methods, which leads to best estimation accuracy. At high SNR, the noise power becomes too small to be accurately estimated. Hence, the measured NMSE increases after the optimal point.

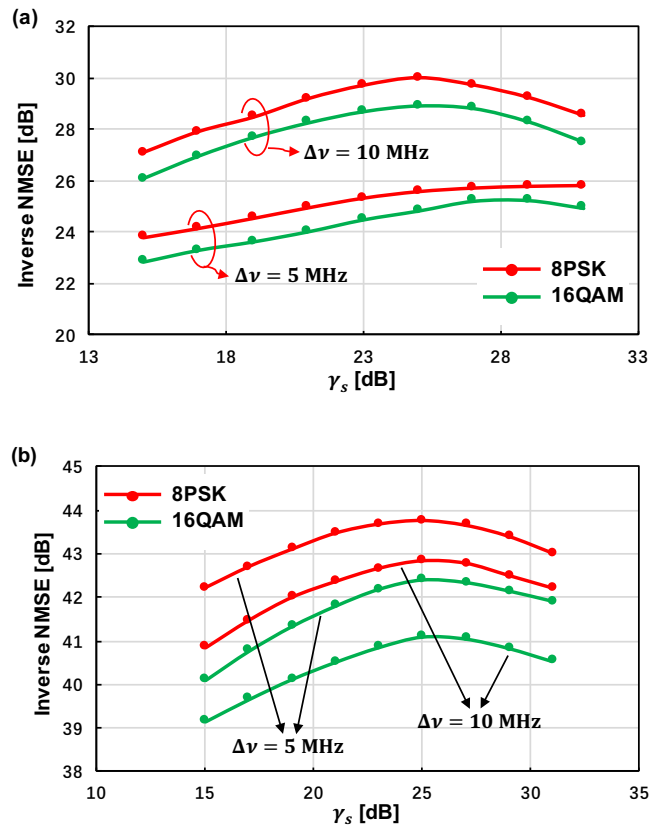


Fig. 5. Performance investigation of (a) filter gain and, (b) decision based SNR estimators.

4.2. Experimental demonstration

An experiment is conducted to verify the performance of the decision based laser linewidth and SNR estimation. Since the decision based method requires no prior knowledge of the channel, it is more appropriate to be implemented in real applications. As shown in Fig. 6, a single-channel, back-to-back, coherent 16QAM system with symbol rate $R = 25$ G Symbols/second is used for evaluation. To achieve tunable laser linewidth, at the transmitter side, the light beam from an external cavity laser (ECL) centered at 1550 nm is phase-modulated according to the laser linewidth emulator introduced in [17]. The modulated light beam is separated and used as both the optical carrier and local oscillator. An IQ modulator driven by an arbitrary waveform generator (AWG) operating at 25 G Samples/second is applied to generate 16QAM modulation. An Erbium-doped fiber amplifier (EDFA) is employed to provide an on/off gain of 10 dB. At the receiver side, the optical signal is detected by an optical hybrid & balanced receiver and sampled by a real-time oscilloscope operating at the sample rate of 50 G Samples/second for off-line DSP. After sampling, the modified constant modulus algorithm (MCMA) for multi-level constellations is applied for the channel estimation and the enhanced adaptive DA-ML is applied afterwards for carrier recovery.

In Fig. 7, the laser linewidth and symbol SNR estimation is plotted as a function of $\Delta\nu$. Compared with the simulation results presented above, the decision-based estimation achieves less effective performance during the experiment which is mainly because of the imperfect channel estimation. As shown, after averaging over 200 single estimates, we achieve a reliable performance for both laser linewidth and SNR with all tested $\Delta\nu$. Considering the laser linewidth estimation, the normalized estimation error decreases from around 0.3 to less than 0.05 with $\Delta\nu$ increases from 500 KHz to 5 MHz. That is to say, the decision based method generates more stable performance at large laser linewidth, which is consistent with the observations from our simulation. This is because, the increase of $\Delta\nu$ leads to a large PRE variance which is easier to be accurately calculated. In terms of the SNR estimation, the normalized error for all single estimates is less than 0.1, which is acceptable in real applications.

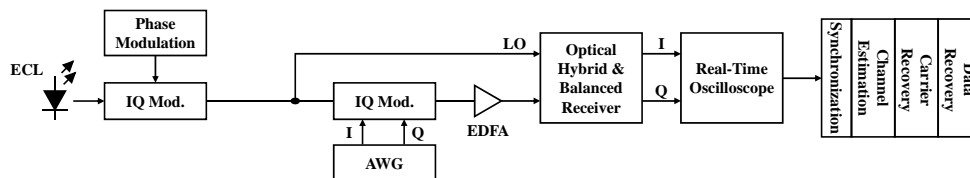


Fig. 6. Experimental setup of the 25 G Symbols/second 16QAM coherent optical transmission system.

5. Conclusion

This paper provides an enhanced adaptive DA-ML carrier phase estimation which outperforms the conventional adaptive phase estimator in terms of both the phase estimation accuracy and the convergence of the actual filter gain to the optimal filter gain. Additionally, this phase estimator provides a means for dynamic measurement of both the laser linewidth and symbol SNR by using either the filter gain or the decision based method. Compared with the conventional DSP based estimation of channel parameters, both filter gain and decision based techniques achieve better performance. Moreover, decision-based techniques require no prior knowledge of the channel parameters which is expected to be efficient in most practical implementations.

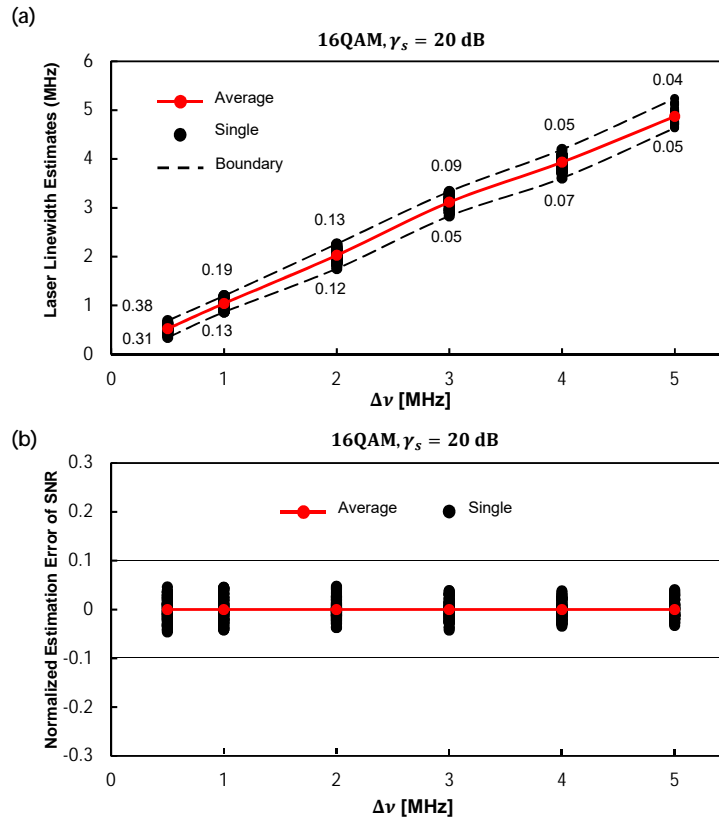


Fig. 7. Experimental evaluation of the performance of the decision based (a) laser linewidth and, (b) SNR estimation.

Funding

AcRF Tier 2 Grant MOE2013-T2-2-135 from MOE Singapore, Grants 61501313, 61471253, 61571316 and 61302112 from the National Natural Science Foundation of China, and Grant 1-ZE5K from HKPU.